# Chapter 2

# Electronic properties of nanostructures

Electronic and optoelectronic devices are shaping our everyday life, ranging from field-effect transistors used in computers and smartphones over the application of light-emitting diodes in displays and screens to photovoltaic cells providing renewable energy. All of these devices are benefiting from nanotechnology, either by a modification of the electronic properties using doping or by using thin-film technology to reduce material consumption, or allowing the use of flexible substrates and large-area production via roll-to-roll processes.

While (opto-)electronic devices rely on semiconductors and their electronic bulk properties, their performance can only be fully understood by taking effects at the nanoscale into account. For example, band bending and the formation of a space-charge region at the interface of a pn-junction formed by combining p- and n-doped semiconductors provides the built-in potential needed for the separation of charges in photovoltaic cells. In addition, interfaces, such as formed between the active layer and the electrodes or within the active layer itself, can limit the efficiency of charge injection or extraction.

The most prominent example for the impact of the on-going miniaturization on the importance of nanostructures and their properties for device performance are field-effect transistors. State-of-the-art transistors in industrial applications exhibit channel lengths of $< 20$ nm, entering the few-atom regime, and even the realization of single-atom transistors has been demonstrated in laboratories. Such small length scales offer opportunities for unprecedented control of the level of impurities and the degree of crystallinity, but also present challenges for the fabrication of structures no longer accessible via well-established lithography methods, and control over the device performance (e.g. short-channel effects).

As the dimensionality of the active layer reduces, the basic electronic properties are fundamentally altered, such that effects unique to nanostructures are observed. The changes are caused e.g. by the variation of the energy-dependence of the density of states with system dimensionality, which in turn directly impacts charge transport and leads to quantization effects in electronic transport. 2D electron gases can be realized at the interface of different materials by band-gap engineering. The energy of the charge carriers is discretized in one dimension, and a constant density of states is

observed. By introducing further lateral constrictions to 2D electron gases, 1D quantum wires or quantum point contacts may be created. Here, at low temperatures electron transport takes place through 1D modes, and conductance quantization occurs. Quasi-0D systems can be realized by using quantum dots, which exhibit a discrete energy system. The so-called Coulomb blockade experienced by electrons transversing the quantum dot leads to charge quantization, such that the passage of individual electrons can be monitored. These distinct properties allow for fascinating basic research, and for broad applications of such nano- to atomic-precision elements.

The observed quantization effects form the basis for the modern practical definitions of the physical units of Ohm and Volt, as discussed in the context of the current definition of the SI units.

The goal of this chapter is to discuss the impact of reduced dimensions on electronic properties focussing on the following aspects:

- Theoretical description of charge transport in bulk materials (single crystals and disordered systems) and the temperature dependence of charge carrier mobilities
- The physics of surfaces and interfaces, including the implications of the existence of a surface on the density of states and electronic bands, the formation of space charge layers and the properties of pn-junctions
- The working principle of standard (opto-) electronic devices such as solar cells, light-emitting diodes and field-effect transistors
- Conductance in low-dimensional systems, from 2D electron gases (including magnetic field effects) to 1D quantum wires and 0D quatum dots
- The role of quantization effects in electronic transport through nanostructures for metrology

## 2.1 Theoretical description of charge transport

Charge transport and the mobility of charge carriers is of fundamental importance for the understanding and the performance of semiconducting devices. In the following, models for the theoretical description of charge transport in different systems are discussed. For details see, e.g., Refs. [K. Seeger "Semiconductor Physics", 2004, Springer Verlag], [D. Jena "Charge Transport in Semiconductors"], [V. Coropceanu et al., Chem. Rev., 2007], [A. Koehler and H. Baessler "Electronic Processes in Organic Semiconductors", Wiley-VCH, 2015]

### 2.1.1 Drude model

In the range of extrinsic conductivity (i.e. the charge carrier concentration $n$ is independent on temperature), the current density $\vec{j}$ caused by applying an external field is given by

$$\vec{j} = n \cdot e \cdot \vec{v_D} \tag{2.1}$$

with the drift velocity $\vec{v_D}$.

In the Drude model, $\vec{v_D}$ is determined from

$$\frac{d}{dt}(m\vec{v}_D) + \frac{m\vec{v}_D}{\langle\tau_m\rangle} = e\vec{E} \tag{2.2}$$

$\langle\tau_m\rangle$ in the second term is the average relaxation time of the charge carriers back to equilibrium. Therefore, this term describes friction the charge carriers experience as they move due to the thermal vibration of atoms, which will depend on the temperature of the crystal.

In the steady state ($d/dt(m\vec{v}_D) = 0$) and for low fields, $\vec{v}_D$ is proportional to the field. We can now define the proportionality constant $\mu$ (the charge carrier mobility) as:

$$\mu = \frac{e}{m}\langle\tau_m\rangle \tag{2.3}$$

With this, the equation for the current density $\vec{j}$ becomes:

$$\vec{j} = \sigma\vec{E} \tag{2.4}$$

with the conductivity $\sigma = n \cdot e \cdot \mu = n\frac{e^2}{m}\langle\tau_m\rangle$

The conductivity $\sigma$ is temperature dependent and can have different origins:

1. Intrinsic, if carriers are generated by thermal excitation
2. Extrinsic, if carriers are generated by introducing dopants
3. Injection controlled, if carriers are injected at electrodes
4. Photoconductivity, if carriers are generated by absorption of light

So far, we discussed the general motion of a charged particle in a material, without considering the crystal structure. We turn now to a discussion of the motion of an electron in the valence band of a perfect semiconductor under the influence of an applied electric field. The discussion of the electron movement in the conduction band can be done accordingly. The general equation of motion of the electron in $k$-space can be written as:

$$\vec{F} = (-e) \cdot [\vec{E} + \vec{v} \times \vec{B}] = \hbar \frac{d\vec{k}}{dt} \tag{2.5}$$

As the electron reaches the end of the 1. Brioullin Zone (BZ) an Umklapp-process takes place, meaning that the electron re-enters the 1. BZ. These Umklapp-processes occur as long as the field is too small to cause the transition of an electron to the next nearest empty band across the energy gap. This transition, which happens at higher fields, is called *Zener tunnelling*, but will not be discussed in more detail here. The force the electron experiences by the applied electric field mainly affects the electron momentum, the velocity and the acceleration of the electron is determined by the band structure.

A typical way of including the band structure in the discussion of charge transport is by introducing an effective mass $m^*$. We can then assume that the electron still moves according to $E = \frac{\hbar^2 k^2}{2m}$ when we replace $m$ by $m^*$, with

$$\frac{1}{m^*} = \frac{1}{\hbar^2} \frac{d^2 E}{dk^2} \tag{2.6}$$

We can now re-do the above calculations of the Drude model, to take into account the band structure and obtain:

$$\mu = \frac{e}{m^*} \langle \tau_m \rangle \tag{2.7}$$

If $m^*$ is larger than $m$ (i.e., if for small bands), the mobility $\mu$ is correspondingly smaller. This is one of the origins of the smaller mobility of organic semiconductors compared to inorganic semiconductors. Although the physics of charge transport in inorganic and organic semiconductors can be discussed using similar models, disorder effects and the lower dielectric constants, effects which will be discussed later in more detail, lead to narrower bands in organic semiconductors.

A complete physical description is given by the Schroedinger equation, but this is too complex and too time consuming for most purposes. Thus, usually simplified models are used to describe charge transport in crystals and we will discuss in the following two of these models.

### 2.1.2 Boltzmann's Transport Equation and drift-diffusion model

The Boltzmann's Transport Equation (BTE) is a general theory to describe the properties of dilute gases by analysing collision processes and has been successfully applied to describe charge transport in highly crystalline systems in which the electrons can be considered as a classical gas.

We briefly summarize the main results and refer the reader to the excellent review by D. Jena "Charge Transport in Semiconductors".

The idea is to use a distribution function $f(\vec{r}, \vec{k}, t)$ to describe the probability of finding an electron at time $t$ at a position $\vec{r}$ with a wavevector $\vec{k} \pm d\vec{k}$. At equilibrium and in the absence of external fields the distribution function is given by Fermi-Dirac statistics.

Any external perturbation drives the distribution function away from equilibrium. This is described by the Boltzmann transport equation (BTE), which is formally written as:

$$\frac{df}{dt} = \frac{\vec{F}_t}{\hbar} \nabla_k f(\vec{k}) + \vec{v} \nabla_r f(\vec{k}) - \frac{\partial f}{\partial t} \tag{2.8}$$

Here, the first term describes the change in the distribution function due to the total force of the field $\vec{F}_t = \vec{E} + \vec{v} \times \vec{B}$ and describes a **drift of the charge carriers**. The second term describes the change in the distribution function due to concentration gradients and corresponds to a **diffusion of the charge carriers**. The last term describes the local change in the distribution function.

The BTE describes how an initial distribution function changes with time due to drift, diffusion and collisions (described by the term $\frac{df}{dt}$). Importantly, since collisions thermalize the distribution function and, thus, drive it back to equilibrium, the contribution to the change in the distribution function has a sign opposite to the contributions from drift and diffusion.

Based on the BTE the temperature dependence of the mobility $\mu$ can be calculated using the expression for the current density $\vec{j}$ introduced in the Drude model, which results in $\mu \propto T^{-n}$ with a positive exponent $n$, thus $\partial\mu/\partial T < 0$. This temperature dependence of the mobility is a fundamental result and describes the temperature dependence of the mobility in ideal (pure) single crystals, where the charge transport can be described by **band transport**.

For most real-life systems the BTE is very difficult to solve, which is the reason why a simplified model was introduced: The drift-diffusion model.

The drift-diffusion model is a semi-classical model and makes the following assumptions:

1. The electrons are treated as classical particles
2. Charge carriers are in local equilibrium (thermalized by electron-electron and electron-lattice interactions)
3. All dopants are ionized
4. Electrical current is the result of two processes: a drift under an applied electric field and diffusion from regions of high charge carrier concentration to low charge carrier concentration

In the following, we will discuss the different contributions to the model.

*1. Drift contribution*
From the Drude-model we know that the drift current $\vec{j}$ due to an applied electric field

$\vec{E}$ can be written as $\vec{j}_{drift} = qn\mu\vec{E}$ for electrons with $q$ the charge, $n$ the density and $\mu$ the mobility.

*2. Diffusion contribution*
Charge carriers diffuse from regions of high concentrations to regions of low concentrations driven by the thermal energy. The diffusion current can be written as $\vec{j}_{diff} = qD\vec{\nabla}n$ with the diffusion constant $D$ and the concentration gradient $\vec{\nabla}n$.

The total current due to drift and diffusion for electrons (charge carrier density $n$) and holes (charge carrier density $p$) is then:

$$\vec{j}_n = qn\mu_n\vec{E} + qD\vec{\nabla}n \quad \text{respectively} \quad \vec{j}_p = qp\mu_p\vec{E} + qD\vec{\nabla}p \tag{2.9}$$

for electrons ($n$) or holes ($p$), respectively.

Importantly, when drift or diffusion occurs, the semiconductor is no longer in thermal equilibrium and there is no common Fermi energy throughout the semiconductor. However, the electron and hole distributions can still be described by the Fermi-Dirac distribution, they are only no longer in thermal equilibrium.

Thus, we introduce the "quasi-Fermi level" $\epsilon_{f,n}$ and $\epsilon_{f,p}$ for electrons and holes:

$$n_c(\vec{r},T) = N_c(T)\exp(-\frac{E_c(\vec{r}) - \epsilon_{f,n}(\vec{r})}{k_BT}) \tag{2.10}$$

and

$$p_v(\vec{r},T) = N_v(T)\exp(-\frac{\epsilon_{f,p}(\vec{r}) - E_v(\vec{r})}{k_BT}) \tag{2.11}$$

Here, $n_c$ and $p_v$ are the concentrations of electrons and holes, $N_c(T)$ and $N_v(T)$ are the DOS in the conduction and valence band and $E_c(\vec{r})$ and $E_v(\vec{r})$ is the conduction and valence band edge. The non-equilibrium conditions which lead to the formation of these "quasi-Fermi levels" are also the origin of the two processes leading to the electric current.

The change in the "quasi-Fermi levels" due to thermalization effects can then be written as:

$$\nabla\epsilon_{f,n}(\vec{r},T) = \nabla E_c(\vec{r}) + k_BT\frac{\nabla n_c(\vec{r},T)}{n_c(\vec{r},T)} \tag{2.12}$$

and

$$\nabla\epsilon_{f,p}(\vec{r},T) = \nabla E_v(\vec{r}) - k_BT\frac{\nabla p_v(\vec{r},T)}{p_v(\vec{r},T)} \tag{2.13}$$

In both equations, the first term corresponds to an electric force $q\vec{F} = \nabla E_{c,v}(\vec{r})$ and describes the drift current. The second term is a force driven by a concentration

gradient, i.e. a diffusion force leading to a diffusion current.

In total, we have

$$\vec{j} = \vec{j}_{drift} + \vec{j}_{diff} = [\sigma_n(T) + \sigma_p(T)]\,\vec{E} + \frac{k_B T}{q}\left[\frac{\sigma_n}{n_c}\nabla n_c - \frac{\sigma_p}{p_v}\nabla p_v\right] \tag{2.14}$$

This leads us back to the Drude model, in which the scattering force is taken into account by a scattering term.

#### 2.1.2.1 Addendum to Eq. 2.14

Restricting the discussion to 1D for simplicity, Eq. 2.14 can be derived from Eq. 2.9 by using the Quasi-Fermi levels. The diffusion constant $D$ can be expressed in terms of the mobility $\mu$ and the charge $q$ using the Einstein-relation (without derivation):

$$D = \mu\frac{k_B T}{q} \tag{2.15}$$

We continue with rewriting $\vec{\nabla} n$ or (for simplicity again in 1D) $\frac{dn}{dx}$ based on the definition of the Quasi-Fermi levels:

$$\begin{aligned}\frac{dn}{dx} &= N_C \frac{d}{dx}\exp\left\{-\frac{E_C - \epsilon_{f,n}}{k_B T}\right\} \\ &= N_C \frac{1}{k_B T}\exp\left\{-\frac{E_C - \epsilon_{f,n}}{k_B T}\right\}\cdot\left\{-\frac{dE_C}{dx} + \frac{d\epsilon_{f,n}}{dx}\right\} \\ &= \frac{1}{k_B T} n\left\{-\frac{dE_C}{dx} + \frac{d\epsilon_{f,n}}{dx}\right\}\end{aligned} \tag{2.16}$$

Analogous, we obtain

$$\frac{dp}{dx} = \frac{1}{k_B T} p\left\{-\frac{d\epsilon_{f,p}}{dx} + \frac{dE_V}{dx}\right\} \tag{2.17}$$

With this, Eq. 2.9 becomes (in 1D):

$$\begin{aligned}\vec{j}_n &= n\mu_n q\vec{E} + qD_n\frac{n}{k_B T}\left\{-\frac{dE_C}{dx} + \frac{d\epsilon_{f,n}}{dx}\right\} \\ \vec{j}_p &= p\mu_p q\vec{E} + qD_p\frac{p}{k_B T}\left\{-\frac{d\epsilon_{f,n}}{dx} + \frac{dE_V}{dx}\right\}\end{aligned} \tag{2.18}$$

Taking now into account that the electric field "shifts" the Fermi-sphere out of the equilibrium position, i.e. $q\vec{E} = \pm\frac{dE_{C/V}}{dx}$ and using the Einstein-relation $D = \mu\frac{k_B T}{q}$ we end up with:

$$\begin{aligned}\vec{j}_n &= \mu_n n\frac{d\epsilon_{f,n}}{dx} \\ \vec{j}_p &= \mu_p p\frac{d\epsilon_{f,p}}{dx}\end{aligned} \tag{2.19}$$

Thus, the gradient of the Quasi-Fermi levels describes the total force acting on the carriers, from both, *drift* and *diffusion*.

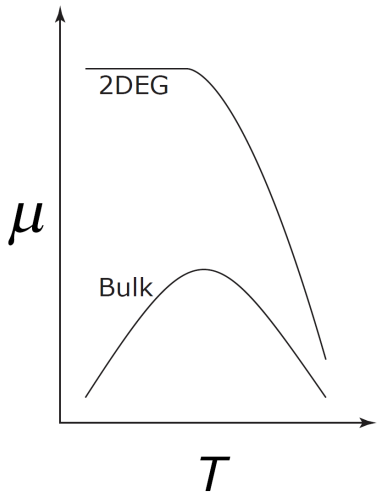


Fig. 2.1: Temperature dependence of charge carrier mobility for a bulk sample and a 2DEG. D. Jena "Charge Transport in Semiconductors" Fig. 6b

### 2.1.3 Temperature dependence of mobility

So far, we have discussed ideal crystals without any defects for which we can describe the electrons with a delocalized wavefunction. Scattering only occurs between the electrons or with the lattice and the mobility decreases with increasing temperature due to increasing scattering with phonons. This will be discussed in the following. The origin on the reduction of mobility at lower temperatures as shown in the picture below will be discussed later.

*1) Scattering at phonons*

Scattering at phonons leads to the decrease in the mobility at higher temperatures. The corresponding scattering process is usually described based on time-dependent perturbation theory. We consider an electron with a wavefunction $\Psi_k$ which scatters at a lattice vibration. This lattice vibration is described as a small perturbation of the crystal potential. The probability that an electron makes a transition from a state with wavevector $\vec{k}$ to a state with wavevector $(\vec{k}')$ as a result of the interaction with the lattice vibration is (in perturbation theory) given by:

$$P(\vec{k},\vec{k}') = \frac{2\pi}{\hbar}\left|M(\vec{k},\vec{k}')\right|^2 \delta(E_{k'} - E_k) \tag{2.20}$$

with the Matrix element:

$$M(\vec{k},\vec{k}') = \int A\Psi^*_{k'}(\vec{r})\Psi_k(\vec{r})V_p d^3r \tag{2.21}$$

and the perturbed crystal potential $V_p$.
Reminder: The mean free path of a charge carrier is $l = \nu\tau$, i.e. the velocity times the

time between collisions. Thus, the collision rate $1/\tau = \nu/l$
For scattering at phonons the collision rate is given by the probability of collision averaged over the volume of the crystal, times the loss in momentum per scattering event (described by a factor $g(\vec{k}, \vec{k'})$) and integrated over all ($\vec{k'}$):

$$\frac{1}{\tau} = \frac{V}{(2\pi)^3}\frac{2\pi}{\hbar}\int \left|M(\vec{k}, \vec{k'})\right|^2 \delta(E_{k'} - E_k) g(\vec{k}, \vec{k'}) d^3k' \tag{2.22}$$

For us, the temperature dependence of the collision rate is the important property and has the following contributions:

1. The matrix element contains a phonon amplitude factor $A$, which takes into account that the occupation number of the phonon modes is temperature dependent (compare BM KoMa), and which is linear in temperature

2. The constant energy surface which is used in the integral to calculate the collision rate is dependent on $k'$ and on the square root of the temperature (see DOS)

This results in a temperature dependence of the collision rate of $\frac{1}{\tau} \propto T^{3/2}$ and (since $\mu = e/m^*\tau$) leads to a temperature dependence of the mobility of $\mu \propto T^{-3/2}$.
Thus, we can conclude that the origin of the reduction of mobility at higher temperatures is scattering at phonons.
For temperatures below 100 K, acoustic phonon scattering dominates, since optical phonons have energies of 30 - 60 meV and are therefore inefficient scatterers at low temperatures. At temperatures above 100 K, scattering at optical phonons has to be taken into account and modifies the temperature dependence slightly ($\mu \propto T^{-1.67}$).

*2) Scattering at ionized impurities (screened Coulomb potential)*

Scattering at phonons is the only origin of a reduction of mobility in ideal, pure crystals. However, in many samples it is observed that with decreasing temperature the mobility decreases again after reaching a maximum. This is due to scattering at impurities and structural defects and we will discuss in the following the scattering processes which lead to the observed temperature dependence of the mobility. The interested reader is referred to Seeger's book for details.
We consider a singly ionized impurity atom of charge $Ze$ fixed inside the crystal. The scattering cross section obtained from classical mechanics (Rutherford scattering) is:

$$\sigma(\Theta) = \left[\frac{K/2}{sin^2(\Theta/2)}\right]^2 \tag{2.23}$$

with $K$ being the distance for which the potential energy equals twice the kinetic energy ($K = Ze^2/(4\pi\epsilon\epsilon_0 mv^2)$). Here, we assume that the Coulomb potential of the impurity extends to infinity.
However, the Coulomb potential has to be modified since the electrostatic field of the individual ionized impurity is screened by the surrounding charge carrier gas. This leads to the formation of screening charges around the impurity and the charge carrier

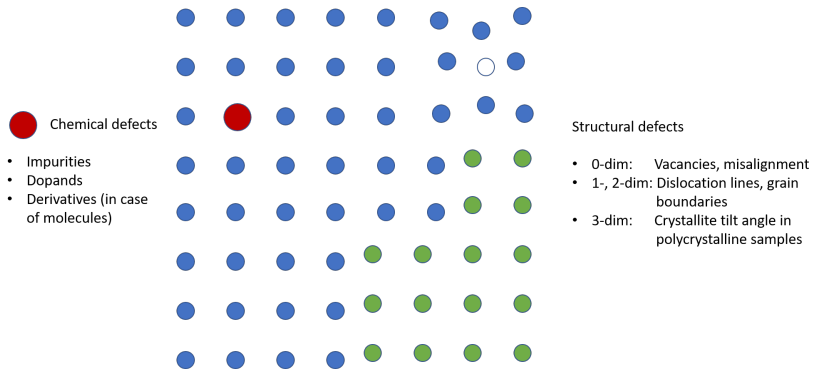


Fig. 2.2: Defects in thin films and crystals.

density in the vicinity of the ionized impurity is different from the averaged carrier density. This can be taken into account by the "screened Coulomb-potential" (Yukawa-potential):

$$V(r) = -\left(\frac{Z\,|e|}{4\pi\epsilon\epsilon_0 r}\right)\exp(-r/L_D) \tag{2.24}$$

Here, we introduced the screening length $L_D$ (Debye-length) to take into account that the electrostatic field of the ionized impurity is screened by the surrounding carriers. Therefore, in the vicinity of an ionized impurity, the density of charge carriers will be $n(r) = n \cdot \exp(-eV(r)/k_BT) \approx n(1 - |e|\,V(r)/k_BT)$.

The corresponding scattering cross section is

$$\sigma(\Theta) = \left[\frac{K/2}{sin^2(\Theta/2) + (2kL_D)^{-2}}\right]^2 \tag{2.25}$$

The effect of the scattering at ionized impurities decreases with increasing temperature due to the thermal velocity ($v_{th} \propto T^{1/2}$), since the charge carriers spend less time in the vicinity of the impurity.
Now we make the important assumption that no scattering occurs unless the electron is close enough ($r_s$ is critical distance) to the ion for the electrostatic potential to be comparable with the thermal energy $V_y(r_s) = \frac{3}{2}k_BT$. This gives a temperature dependence of $r_s \propto T^{-1}$ and a temperature dependence of the scattering cross section $\sigma = r_s^2\pi \propto T^{-2}$.
Reminder: $\tau_{th} \propto \frac{l}{v_{th}} \propto \frac{l}{T^{1/2}}$ with $l$ the mean free path and $l \propto \frac{1}{\sigma}$ (proportional to the scattering probability).
This results in $\tau \propto \frac{1}{\sigma}\frac{1}{T^{1/2}} \propto T^2 \cdot T^{-1/2} = T^{3/2}$ and, finally, $\mu = \frac{e}{m}\tau \propto T^{3/2}$.

From this, we can conclude that at low temperatures the mobility in bulk semiconductors is limited by scattering at ionized impurities.

### 2.1.4 Charge transport in disordered materials

In general, low energy sites, which can lead to localisation of the charge carrier wavefunction or lead to scattering of the charge carriers, are called trap states. In inorganic

as well as in organic semiconductors, such trap states are for example impurities (neutral or ionized) or structural imperfections of the crystal lattice.

We have already seen before that the DOS will depend on the dimensionality of the system. In organic semiconductors, the extent of electronic delocalization depends on the strength of the electronic coupling between molecules as well as the energetic and positional disorder, which we will discuss later and which leads to electronic localization.

Organic semiconductors display a wide range of long-range order, from highly crystalline samples such as single crystals of pentacene or rubrene to polycrystalline or even amorphous thin films.

Depending on the sample preparation procedure, polycrystalline and amorphous domains can coexist in one sample. In combination with energetic disorder due to chemical impurities, grain boundaries or crystal defects, electron-phonon interactions and the low dielectric constant in organic molecules results in weak Coulomb screening and high electronic localization. This results in a narrow bandwidth of $< 500$ meV.

In addition, the weak Coulomb screening leads to strong binding energies between electrons and holes and to the formation of exciton states. This has important implications for charge transport and the functioning of optoelectronic devices such as solar cells or light emitting diodes, which will be discussed in following chapters. In contrast, due to the large dielectric constant of inorganic semiconductors and the high Coulomb screening, the binding energy of excitons is in the order of the thermal energy and therefore, they can easily be dissociated even at room temperature.

In the following, we will discuss briefly how long-range order affects the density of states and accordingly, the theoretical models which can be used to describe charge transport. In crystalline solids, electronic wave functions overlap significantly, and electronic bands are formed with energy gaps in between due to the symmetry of the unit cells. The presence of defects or dopants leads to the occurrence of localized states within the band gap which can act as traps or as doping sites creating free charge carriers. The electronic and optical properties of such crystalline solids can be well described with band theory. Band theory is a one-electron independent particle theory that assumes the existence of a set of stationary extended one-electron states distributed according to the Fermi-Dirac distributions. Polycrystalline solids consist of crystalline grains which are separated by grain boundaries. These grain boundaries and other defects such as impurities or lattice dislocations introduce localized electronic states in the energy gap for which the wave function of the electron only extends over a few nearest neighbouring atoms. If the material has a lot of grain boundaries or other defects, a continuum of localized tail states can form, which is often observed in organic semiconductors. These tail states are obviously important for devices, in particular for field effect transistors with low gate voltages, since by varying the gate voltage the Fermi level is moved through the DOS. Finally, in amorphous solids we only have short range order and accordingly, the electronic wave function only extends over a few nearest neighbours. This results in narrow bandwidths and there is also a continuum of localized and extended tail states observed due to disorder induced localised states. These materials cannot longer be described by band theory and other models have to be used.

In materials with significant degrees of disorder, charge transport cannot be described by band transport, but involves incoherent electron transfer reactions, which strongly depend on the electronic coupling. The coupling between two localized states $|\Psi_a\rangle$ and $|\Psi_b\rangle$ is described by the transfer matrix element $t_{ab} = \langle\Psi_a|H|\Psi_b\rangle$, where $H$ is the Hamiltonian of the system.

There are several, very successful models which incorporate energetic disorder to describe charge transport. We will briefly introduce the most common model, the Gaussian Disorder Model developed by Baessler and co-workers. As for many other models (such as e.g. the famous Marcus model), it is assumed that the hopping sites are distributed following a Gaussian distribution of the DOS with a standard deviation $\sigma_{DOS}$.

Hopping occurs between non-equivalent sites $e_i$ and $e_j$ within this Gaussian DOS, which are randomly selected.

The model is based on a few reasonable assumptions about the disorder.

- Energies of defect electrons or transport states exhibit a Gaussian distribution of DOS
- The hopping rate is given by the product of the Boltzmann factor, a pre-exponential factor and a factor that takes into account the overlap of the wave-functions (which is (also) not sharp, but subject to a distribution)

The central result is that for small electrical fields the mobility behaves as

$$\mu = \mu_0 \exp(-(T/T_0)^2) \tag{2.26}$$

with $T_0 = (2\sigma)/(3k_B)$.

Importantly, this model disregards polaronic effects which we will discuss in the following.
Adding a free charge carrier in an organic solid leads to the deformation of the molecular geometry. This can be understood in the Frank-Condon picture in which the minimum of the electronic ground state and the electronic excited state are not at the same configurational coordinate. Therefore, the molecule has to deform slightly to find the energetically lowest configuration when a charge is placed on the molecule. The energy necessary for this deformation is called the *reorganisation energy,* $\lambda_{int}$.

In addition to changes in the molecular configuration, the whole lattice, i.e. the surrounding molecules will react to the charge on the molecule. When the charge moves to the next molecule, the lattice deformation will follow this movement, resulting in a coupling of the charge carrier to the lattice vibration (=phonon) and a second contribution to the reorganisation energy, $\lambda_{ext}$.

The quasiparticle corresponding to this coupled state of charge carrier and phonon is called *polaron* and dominates the charge transport in organic semiconductors. The

reorganization energy describes the polaron binding energy.

A polaron describes a charge carrier surrounded by a polarized medium and therefore, the effective mass of this quasiparticle will be larger than the effective mass of a free charge carrier in an inorganic solid. The larger the effective mass of the polaron, the more localized is its wavefunction. In organic semiconductors, polarons are usually highly localized and referred to as small polarons.

The polaron binding energy is $\lambda_{reorg} = \lambda^1_{int} + \lambda^2_{ext}$ and results from the deformation in molecular geometry and lattice geometry as the carrier localizes on a given site.

Such polarons can move between equivalent localized polaron states by tunnelling or by hopping between non-equivalent sites, which requires the absorption or emission of a phonon. Tunnelling of polarons results in band-like behaviour and usually dominates at low substrate temperatures. Hopping is a thermally activated process and thus, dominates at higher temperatures.

In summary, these are the quantities, which determine charge transport in highly disordered systems:

- Transfer integral: Looking at electron (charge) transfer processes, the transfer integral describes the "interaction" of wavefunctions of the two molecules involved in the charge transfer process, i.e. the electronic coupling.
- Reorganization energy: Tends to localize charge and has two contributions, an internal (Energy necessary to accommodate charge on molecule) and an external (Energy necessary for local environment to react to change in polarisation)

The most successful model in describing polaronic transport is the *Holstein model*, which uses perturbation theory to calculate an electron transfer rate in the hopping regime, which will depend on the temperature T and the energy of the phonon $\hbar\omega$ to which the electron couples. Importantly, this theory excludes the existence of disorder!

The central result is that hopping transport is described by three regimes:

- Tunnelling regime: Coherent electron transfer processes. The mobility exhibits a band-like temperature dependence. This dominates at low temperatures
- Hopping regime: Incoherent electron transfer processes dominate above a critical temperature $T_1$. These electron transfer processes are field-assisted and thermally activated and only involve nearest neighbours. The mobility shows an activation behaviour.
- Electron scattering regime, the polarons are dissociated and the charge carriers are scattered at thermal phonons, leading to a decrease in mobility with increasing temperature.

Finally, we will discuss the crossover from band to hopping transport, which is in the Holstein model determined by the strength of electron phonon coupling:

- In case of weak electron-phonon coupling, the mobility will be dominated by coherent electron transfer processes and display a band-like transport behaviour in which the mobility increases with decreasing temperature.
- In case of medium electron-phonon coupling, bandlike transport dominates a low temperatures, but due to the hopping contribution it will exhibit a weaker temperature dependence at higher temperatures.
- In case of strong electron-phonon coupling we are back at the three regimes discussed before.

As a final note: Although the Holstein model is very useful in the description of charge transport, it explicitly doesn't include disorder and therefore, cannot be a complete model of charge transport. There are more sophisticated attempts for a description of charge transport, for example the effective medium model or the multiple trapping and detrapping model, but a discussion of those models exceeds the scope of the lecture.

## 2.2 Electronic structure of surfaces and interfaces

Especially for the understanding of devices, an understanding of differences in the electronic structure of surfaces and interfaces compared to the bulk is of high importance. Refs. [K. Seeger "Semiconductor Physics", 2004, Springer Verlag], [H. Lueth "Solid surfaces, interfaces and thin film", 2010, Springer], [J. Singh "Semiconductor devices-Basic Principles" Chapter 7 (www.eecs.umich.edu/ singh)]

### 2.2.1 Surfaces

The electronic properties of a surface can be quite different from the properties of the bulk. This is caused by impurities, i.e. missing atoms, surface reconstruction, dangling bonds or, very generally speaking, by the break in the crystal symmetry.
The challenge in the theoretical description of a surface is that even in the ideal case the translational symmetry only exists in directions within the plane of the surface. Because of changed chemical bonding near the surface, the surface may relax and reconstruct, leading to a displacement of atoms from their "ideal" bulk positions. All these effects lead to the occurrence of electronic surface states which will be discussed in the following.

#### 2.2.1.1 Electronic surface states (simple chain model): Shockley states

Start with a 2D surface of an ideal crystal and assume that the electrons are nearly free. In a simplified treatment, we model the bulk by a semifinite chain and the surface as the end of the chain.
The potential V along the chain is assumed to follow a cosine-function as expected for the free electron model:

$$V(z) = \hat{V}\left[\exp\left(\frac{2\pi i z}{a}\right) + \exp\left(\frac{-2\pi i z}{a}\right)\right] = 2\hat{V}cos\left(\frac{2\pi z}{a}\right) \tag{2.27}$$

Here, $\hat{V}$ is a constant, $z < 0$ and $a$ is the distance between the atoms.
We describe the surface (at $z = 0$) as an abrupt change in the potential (a step to $V_0$). Solving now the Schroedinger-equation:

$$\left[-\frac{\hbar^2}{2m}\frac{d^2}{dz^2} + V(z)\right]\Psi(z) = E\Psi(z) \tag{2.28}$$

For regions deep within the bulk ($z \ll 0$) we can consider the chain to be infinite and neglect surface effects. In this case, we can assume a periodic potential ($V(z) = V(z+na)$) and obtain as solution the well-known Bloch waves ($\hat{V}$ and $C$ are constants):

$$\Psi_i = Ce^{i\kappa z}\left\{e^{i\pi z/a} + \frac{\left|\hat{V}\right|}{\hat{V}}\left[\frac{-\hbar^2\pi\kappa}{ma\left|\hat{V}\right|} \pm \sqrt{\left(\frac{\hbar^2\pi\kappa}{ma\left|\hat{V}\right|}\right)^2 + 1}\right]e^{-i\pi z/a}\right\} \tag{2.29}$$

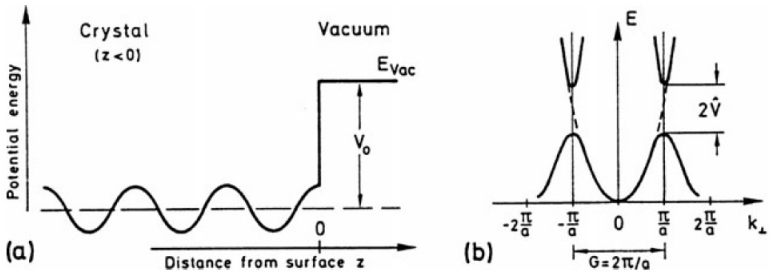


**Fig. 6.1 a,b** Nearly-free-electron model for a cosine potential along a linear chain ($z$-direction). (**a**) Potential energy in the presence of a surface at $z = 0$. (**b**) Energy bands $E$ ($k_\perp$) for one-electron bulk states

Fig. 2.3: Figure from H. Lueth: Solid surfaces, interfaces and thin films, Springer (2010).

For us, solutions near the surface of the crystal ($z = 0$) are now more interesting. These solutions have to fulfill three condititions:

- They have to be compatible with $E_{vac} = V_0 = const$ for $z > 0$
- They have to solve the Schroedinger equation for the crystal side ($z < 0$)
- Both solutions ($\Psi$ and $\frac{\partial \Psi}{\partial z}$) have to match at $z = 0$.

The solution in the constant potential $V_0$ on the vacuum side for $z > 0$ has to be exponentially decaying.

$$\Psi_0 = D \exp\left[-\sqrt{\frac{2m}{\hbar^2}(V_0 - E)}z\right] \tag{2.30}$$

with $E < V_0$. The solution for $z \ll 0$ and $z > 0$ can only match if by superimposing an incoming and a reflected wave near the surface (standing wave) the solution of $\Psi_0$ does not contain a complex contribution. The matching condition is:

$$\Psi_0(z = 0) = \alpha\Psi_i(z = 0, \kappa) + \beta\Psi_i(z = 0, -\kappa) \tag{2.31}$$

Possible solutions are standing Bloch waves in the crystal which are matched to exponentially decaying tails on the vacuum side (Fig. 2.3 (a)). Importantly, electronic energy levels are only slightly modified from those of the bulk crystal.

If we now allow for complex wave vectors ($\kappa = -iq$), additional solutions are possible and result in a standing wave with exponentially decaying amplitude (Fig. 2.4). For details of the derivation we refer the interested reader to the book by Lueth. The resulting states are the **surface states**.
The matching conditions at the surface lead to two effects:

1. The electrons in these states are localized within a couple of Å of the surface plane.

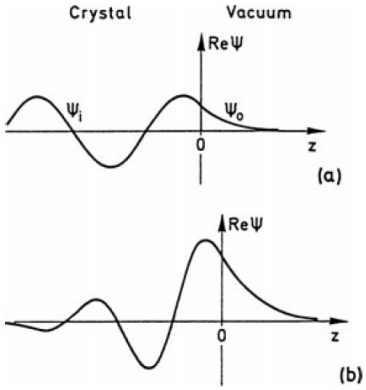


**Fig. 6.2** Real part of the one-electron wavefunction, Re{$\psi$}, for (**a**) a standing Bloch wave ($\psi_i$), matched to an exponentially decaying tail ($\psi_0$) in the vacuum; (**b**) a surface-state wave function localized at the surface ($z = 0$)

Fig. 2.4: Figure from H. Lueth:Solid surfaces, interfaces and thin films, Springer (2010).

2. The allowed energy values are restricted and the energy of a surface state lies within the gap of the bulk states, i.e. within the energy gap of the crystal.

Surface states of ideal clean surfaces of the near-free electron model are called **Shockley-states**.

#### 2.2.1.2 Electronic surface states (tight binding approximation): Tamm states

An alternative approach is to start from the tight binding approximation and to apply the method of LCAO (linear combination of atomic orbitals). The starting point are tightly bound electrons and the emergence of bands is explained by wavefunction overlap of neighboring atoms in the bulk. The existence of surface states is then easily understood by the existence of dangling bonds at the surface (i.e. atoms which are missing a bonding partner on one side). The splitting and shift of the atomic levels is thus smaller at the surface than in the bulk. The greater the disturbance by the surface, the larger the deviation of the energy of the surface states from the bulk states.

Energetically higher lying surface states have **conduction-band character**, whereas energetically lower lying surface states have **valence-band character**. Since a semiconductor is neutral when all conduction band states are empty and all valence band states are occupied, these surface states have charging character:

- Acceptor-like states are neutral when they are unoccupied, and negatively charged when they are occupied.
- Donor-like states are positively charged when they are unoccupied and neutral when they are occupied.

#### 2.2.1.3 Other surface states

**Extrinsic surface states:** The surface states discussed so far are mainly arising from the break in symmetry at the surface and are still tightly connected to the bulk properties. There are also surface states which arise from imperfections:

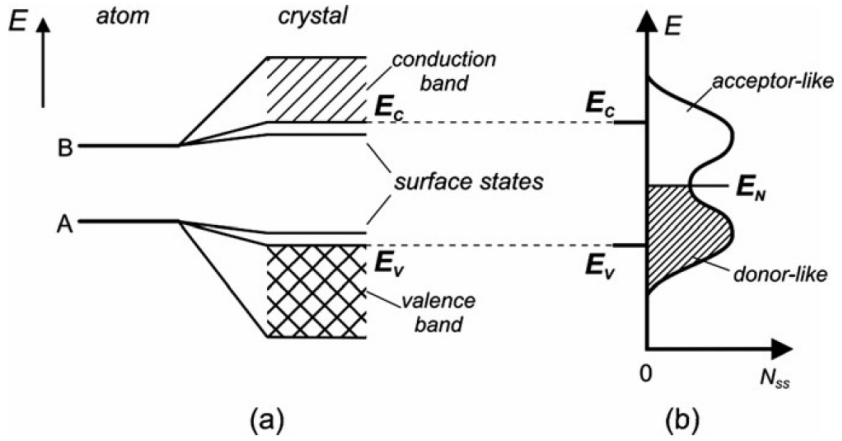


**Fig. 6.5** Qualitative explanation of the origin of surface states in the tight-binding picture. (**a**) Two atomic levels A and B form the bulk valence and conduction bands, respectively. Surface atoms have fewer bonding partners than bulk atoms and thus give rise to electronic energy levels that are closer to those of the free atoms, i.e. surface state levels are split off from the bulk bands. Depending on their origin, these states have acceptor- or donor-like charging character. (**b**) Mostly these (intrinsic) surface states having the periodicity of the 2D surface show dispersion in the surface 2D reciprocal space which results in broader bands of the surface state density $N_{ss}$

Fig. 2.5: Figure from H. Lueth: Solid surfaces, interfaces and thin films, Springer (2010).

- Missing surface atoms can act as traps for charge carriers (esp. in ionic bonds such as ZnO)
- Line defects, such as steps, lead to differences in the atomic environment
- Adsorbed atoms can cause changes in the atomic environment as well

Importantly, these extrinsic surface states do not exhibit 2D translational symmetry in contrast to intrinsic surface states.

**Image potential states at metal surfaces:** Image potential states are of importance for photoelectron spectroscopy. As an electron approaches a metal surface its charge gets screened by conduction electrons. This screening can be described by a positive charge inside the metal at the same distance from the surface as the electron outside, leading to an attractive force. The potential is often approximated as $V(z) \propto z$ for $z > 0$. These states can act as trap states within a couple of Å of the surface. Importantly, they are not derived from bulk states nor are they resulting from the symmetry breaking effects of the surface.

#### 2.2.1.4 Space charge layers at semiconductor surfaces, band bending

Imagine putting a point charge into a locally neutral electron plasma (electrons on background of fixed positive cores). The electrons in the neighborhood will rearrange to compensate that additional charge leading to a screening so that away from the charge the E-field vanishes.
The higher the electron density, the shorter the screening length:

- Metals: Electron concentration $10^{22}\ cm^{-3}$ (screening length: a few Å)

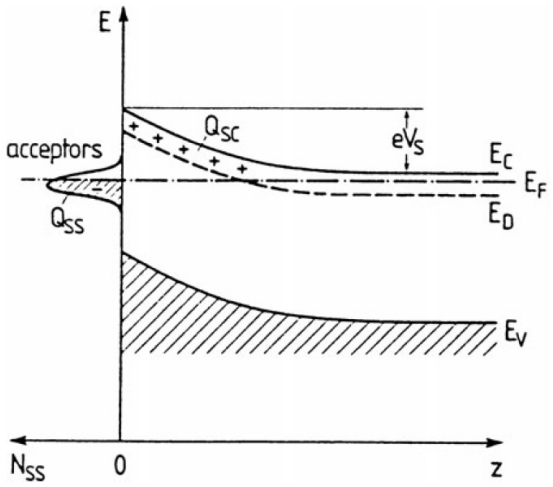


**Fig. 7.1** Band scheme (band energy $E$ versus $z$ coordinate normal to the surface $z = 0$), for an $n$-doped semiconductor with depletion space-charge layer at low temperature (bulk donors not ionized). Partially occupied acceptor type surface states (density $N_{ss}$) are also indicated. Their charge $Q_{ss}$ is compensated by the space charge $Q_{sc}$. $E_F$ is Fermi energy, $E_C$ and $E_V$ conduction- and valence-band edges, respectively, and $E_D$ the energy of the bulk donors. The band bending at the surface is $eV_s$ with $e$ being the positive elementary charge

Fig. 2.6: Figure from H. Lueth: Solid surfaces, interfaces and thin films, Springer (2010).

- Semiconductors: Electron concentration $10^{17}\ cm^{-3}$ (screening length: several 100 Å)

These spatial regions of redistributed screening charges are called space charge regions.

In semiconductors with electronic surface states the local charge balance is disturbed. Depending on the type of the surface state (donating or accepting) and on the position of the Fermi level at the surface, the surface state may carry charge which is screened by charges inside the semiconductor. Let us now assume that we have a surface state with charging character. The position of the Fermi level is given by charge neutrality conditions and thus, the charge of the surface states $Q_{ss}$ is compensated by charges inside the semiconductor. This latter charge screens $Q_{ss}$ and we can write for the space charge $Q_{sc}$: $Q_{ss} = -Q_{sc}$.
**The formation of this space charge layer results in band bending.**

The band bending effect can be understood as follows:

- Deep in the bulk, the position of the Fermi level with respect to the bulk conduction band depends purely on the bulk doping level
- Surface states are inherently related to the existence of a surface. Their position with respect to the conduction band is fixed and determined by the interatomic potential at the surface
- Flat bands up to the surface would result in a Fermi level far above the surface states. This would lead to surface states completely filled with electrons and therefore, a considerably uncompensated charge density would build up. This scenario is energetically unstable and leads therefore to band bending.

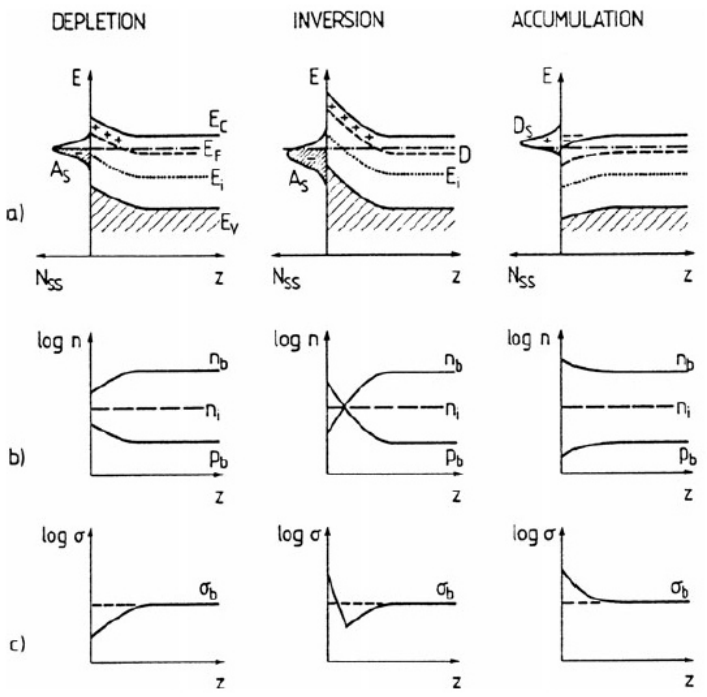


**Fig. 7.2 a–c** Illustrating the $n$-type semiconductor: Schematic plots of band schemes (**a**), free carrier densities $n$ and $p$ on a logarithmic scale (**b**) and local conductivity $\sigma$ (logarithmic scale) (**c**) for depletion, inversion and accumulation space charge layers at low temperature (bulk donors not ionized). $E_C$, $E_V$ are the conduction- and valenceband edges, $E_F$ the Fermi energy, $E_i$ and $n_i$ intrinsic energy and concentration, respectively. $D$ denotes bulk donors, $A_s$ and $D_s$ surface acceptors and donors, respectively. The subscript b denotes bulk values

Fig. 2.7: Figure from H. Lueth: Solid surfaces, interfaces and thin films, Springer (2010).

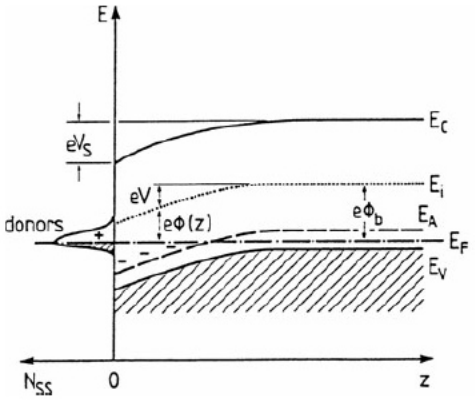


**Fig. 7.3** Band scheme of a hole depletion space-charge layer on a *p*-doped semiconductor at low temperature (bulk acceptors not ionized). $eV_s$ is the band bending at the surface, $eV(z)$ the local band bending, $\phi(z)$ the local potential and $\phi_b$ the potential in the bulk. $E_i$ is the intrinsic energy, $E_F$ the Fermi energy, $E_A$ the energy of bulk acceptors and $E_C$ and $E_V$ as in Fig. 7.1

Fig. 2.8: Figure from H. Lueth: Solid surfaces, interfaces and thin films, Springer (2010).

### Three scenarios of band bending

- Depletion: Distribution of $Q_{sc}$ is related to the curvature of the electronic bands (i.e. potential in space charge layer). Due to the band bending, free conduction band electrons are pushed away from surface and density lowered with respect to bulk density $n_b$. In n-type semiconductor with bulk donors depletion layer is related to decrease in density of free electrons and increase of hole density.

- Inversion layer: Higher densities $N_{ss}$ of surface states at lower energies can lead to even stronger upwards band bending. Because of a greater amount of negative $Q_{ss}$ more bulk donors must be ionized and space charge layer reaches deeper into semiconductor. If we define the intrinsic energy as $E_i = 1/2(E_C + E_V) - 1/2kTln(N^c_{eff}/N^v_{eff})$ with $N_{eff}$ the effective DOS in CB and VB, a semiconductor is *intrinsic* if $E_F = E_i$, it is $n-type$ if $E_F > E_i$ and $p-type$ if $E_F < E_i$. In the inversion layer the type of conduction changes!

- Accumulation layer: Presence of surface states at high energies which are partially empty and thus carry positive surface charge $Q_{ss}$. This charge must be compensated by negative space charge inside the crystal. Thus, free electrons accumulate in the conduction band below the surface.

The difference between a depletion and an accumulation layer is that in the depletion layer the positive space charge originates from spatially fixed ionized bulk donors, whereas in the accumulation layer the negative space charge is due to free electrons which are mobile.

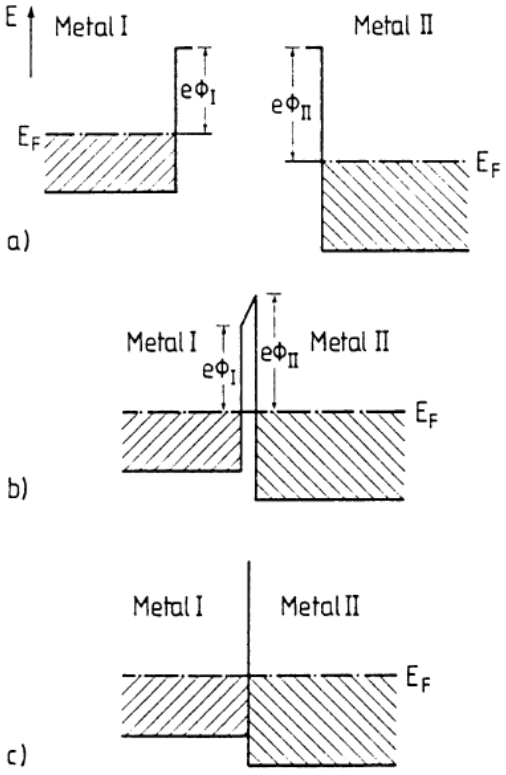


**Fig. 8.1 a–c** Schematic diagram of the formation of a metal–metal interface. **(a)** Simplified band schemes of the two metals I and II with work functions $e\phi_{\mathrm{I}}$ and $e\phi_{\mathrm{II}}$; the metals are assumed to be not in contact with each other; $E_{\mathrm{F}}$ is the Fermi energy. **(b)** Band schemes of the conduction bands at the interface for the two metals in contact. **(c)** Simplified representation of the metal–metal contact; the dipole layer at the interface is not shown

Fig. 2.9: Figure from H. Lueth: Solid surfaces, interfaces and thin films, Springer (2010).

**Quantative description of the space charge layer:**
Maxwell equation: $\mathrm{div}E = \frac{\rho(x)}{\epsilon\epsilon_0}$
$\rho$ (space charge density) gives with $E = -\mathrm{grad}\phi$ the **Poisson equation** in one dimension (perpendicular to the surface):

$$\frac{d^2\phi}{dx^2} = -\frac{\rho(x)}{\epsilon\epsilon_0} \tag{2.32}$$

with $0 < x < \infty$.
The space charge density $\rho(x) = e[N_d^+(x) - N_a^-(x) + p(x) - n(x)]$ results from the densities of ionized donors ($N_d^+$), ionized acceptors ($N_a^-$), holes in the valence band ($p$) and electrons in the conduction band ($n$).

### 2.2.2 The metal-metal interface

When we bring two metals (with work functions $e\Phi_1$ and $e\Phi_2$) in contact, the chemical potential (and the Fermi energy) has to be the same on both sides of the interface in equilibrium. This leads to an alignment of the Fermi levels.

The alignment happens by flow of electrons from the metal with lower workfunction (1) to the metal with higher work function (2). This results in a space charge which is positive in (1) and negative in (2) and leads to the formation of an interface dipole layer.

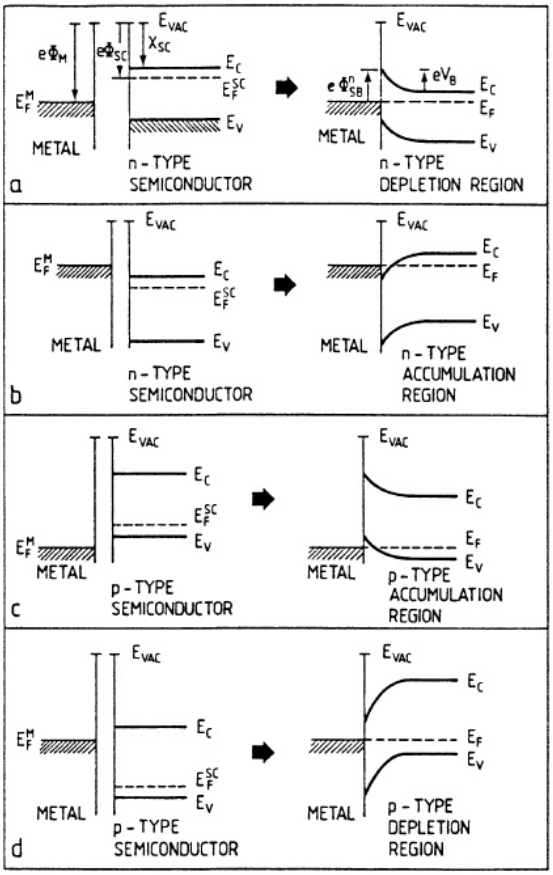


**Fig. 8.2 a–d** Schematic diagrams of band bending before and after metal–semiconductor contact: (**a**) High-work-function metal and *n*-type semiconductor, (**b**) low-work-function metal and *n*-type semiconductor, (**c**) high-work-function metal and *p*-type semiconductor, and (**d**) low-work-function metal and *p*-type semiconductor [8.3]

Fig. 2.10: Figure from H. Lueth: Solid surfaces, interfaces and thin films, Springer (2010).

The size of the dipole layer can be estimated by the screened potential of a point charge: $\Phi(r) = (Q/r)e^{-r/r_{TF}}$, with $r_{TF}$ the Thomas-Fermi screening length: $r_{TF} = 0.5(n/a_0^3)^{-1/6}$ ($n$ electron density, $a_0$ Bohr radius).

### 2.2.3 The metal-semiconductor interface

Also in case of metal-semiconductor interfaces, the Fermi levels have to align. Depending on the work function of the metal $e\Phi$ and the electron affinity of the semiconductor $\chi$, different scenarios can be imagined in a very simple picture.

When brought into contact, charges begin to flow and a dipole layer builds up. The participating charge is screened within a few Å in the metal but in the semiconductor the screening length is much larger and an accumulation or depletion layer is formed.

**1) High work function metal and n-type semiconductor (Schottky barrier)**

- Electrons flow from semiconductor to metal
- A depletion region is formed

- Upward band bending
- Positive space charge of ionized donors

Maximum band bending at the interface is related to the Schottky barrier (potential barrier) the electron has to overcome to go from the metal to the conduction band of the semiconductor.
The Schottky barrier $e\Phi_{SB}$ arises from the alignment of Fermi levels and is given by the difference in Fermi energy of the metal and the electron affinity of the semiconductor (which describes the edge of the conduction band, see Figure): $e\Phi_{SB} = e\Phi_M - \chi_{SC}$.
The built-in potential $eV_B$ is given by the space charge layer that forms due to the electron flow related to the Fermi level alignment and results from band bending. It can be calculated using the height of the Schottky barrier as a measure of the difference between Fermi level and conduction band edge after contact (which gives the energy of the electrons directly at the surface) and subtracting the difference between Fermi level and conduction band edge deep in the bulk (which gives the energy of the electrons in the bulk outside of the space charge layer): $eV_B = e\Phi_M - \chi_{SC} - (E_C - E_F)$.
The current voltage characteristics does not follow an ohmic behaviour, as we will discuss in the next section.

**2) Low work function metal and n-type semiconductor (ohmic contact)**

- Electrons flow from metal to semiconductor
- Accumulation / inversion region is formed
- Downward band bending
- Negative space charge of ionized acceptors

The current voltage characteristics follows Ohm's law: $U = RI$.
The discussion of metal and p-type semiconductor interfaces can be done accordingly.

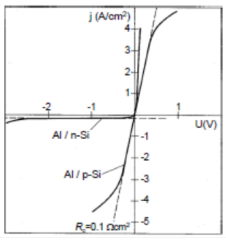


**Beispiel: Al auf Si**
ohmscher Kontakt läßt sich mit $p$-Si wesentlich einfacher realisieren als mit $n$-Si

Fig. A.6: Ohmscher Al/p-Si- und Schottky-Al/n-Si-Kontakt. [nach Bergmann-Schaefer, Lehrbuch der Experimentalphysik, Bd. 6, Festkörper (1992); Abb.6.34].

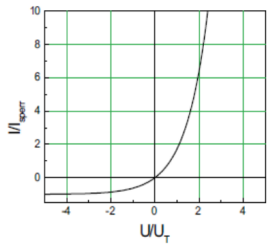


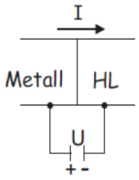


Richardson-Gl.:

$$I(U) = \underbrace{const \cdot e^{-\Phi_n/eU_T} \cdot T^2}_{I_{sperr}} \cdot [e^{U/U_T} - 1] \tag{A.32}$$

mit $U_T \equiv k_B T/e$

Fig. A.8: Strom-Spannungs-Kennlinie eines Schottky-Kontakts.

Fig. 2.11: Schottky contact.

#### 2.2.3.1 Schottky barrier under external voltage (rectifying behavior)

1. No external voltage ($U = 0$): Electrons on side of semiconductor have to be thermally activated to overcome barrier. This leads to a thermionic emission current which flows from the semiconductor to the metal. This thermionic emission current is compensated by an electron current from the metal to the semiconductor. The total current is $I = 0$.

2. $U > 0$ (raises $E_F$ in an n-doped semiconductor): Applying an external voltage in forward direction leads to a reduction of the barrier the electrons travelling from the semiconductor to the metal have to overcome. Since the electrons in the conduction band of the semiconductor obey the Boltzmann statistics, the number of electrons to overcome the barrier depends exponentially on the height of the barrier: $I(U) = I_0(\exp(eU/kT) - 1)$. The saturation current $I_0$ depends on assumptions regarding the carrier transport (thermionic emission, diffusion...)

3. $U < 0$ (lowers $E_F$ in an n-doped semiconductor): This leads to an increase of the barrier the electrons travelling from the semiconductor to the metal see and we only observe the current from the metal to the semiconductor (which depends for $U \ll 0$ only on the height of the Schottky barrier).

Important notice: Electrons moving from the metal to the semiconductor always see the Schottky barrier $e\Phi_{SB}$, whereas the electrons moving from the semiconductor to the metal see a barrier due to band bending of $eV_{eq}$ (in equilibrium).

### 2.2.4 The semiconductor-semiconductor interface, pn-junction

In contrast to metal-semiconductor interfaces, two length scales are important at semiconductor-semiconductor interfaces:

1. The interface dipoles due to the flow of charges across the interface which are formed on an atomic scale
2. The space charge layers which lead to band bending and which extend in semiconductors several hundred Å into the bulk due to the lower charge carrier density.

The most relevant semiconductor-semiconductor interface is the interface between an n-doped and a p-doped semiconductor, the pn-junction. As for the metal-semiconductor interface the following effects are important for an understanding of the semiconductor-semiconductor junction:

1. Energy level alignment, which relates to the band offset ($\Delta E$), which is the difference between the maximum of the valence band and the minimum of the conduction band
2. The band bending, which is a result of the Fermi level alignment, in thermal equilibrium. This can be described using space charge theory as discussed before, if we keep in mind that the junction has to be current free in thermal equilibrium and that the doping determines the position of the Fermi level deep inside the semiconductor.

For the description of the pn-junction (which was first described by W. Shockley in 1949) we assume that the transition between the two regions (p-doped and n-doped) is abrupt, which is in reality not correct, but allows to derive the most important relations, in particular the current-voltage characteristics.
We make the following assumptions:

1. The density of donors $N_D$ (on n-side) and acceptors $N_A$ (on p-side) is constant.
2. All dopants (donors and acceptors) are ionized: $N_D = N_D^+$ and $N_A = N_A^-$

Once the p-doped and the n-doped semiconductor are brought into contact, the Fermi levels align, leading to diffusion of holes from the p-side to the n-side and electrons from the n-side to the p-side and the formation of a space-charge region (depletion-region) at the interface.
Here, the concept of *majority charge carriers* becomes important. The majority charge carriers are holes in a p-doped semiconductor and electrons in an n-doped semiconductor. The holes diffusing to the n-side (and electrons to the p-side) recombine there with the respective majority charge carriers (electrons for n-side and holes for p-side), leading to the formation of a quasi-neutral region on both sides of the space charge region at the interface.
This diffusion current $I_r$ is therefore also called **recombination current**.

As discussed before, this space charge region is formed by stationary ionized dopands (negatively charged acceptors in the p-region and positively charged donor in the n-region), and the spatial extent of the space charge region is defined by the Debye screening length $L_D$, here shown for a semiconductor surface. The width of the space charge region across the pn-junction is given below.

$$L_D = \sqrt{\frac{2\epsilon\epsilon_0\Psi_S}{\rho_0}} \propto \frac{1}{\sqrt{\rho_0}} \tag{2.33}$$

Here, $\Psi_S = \Phi_{surf} - \Phi_b$ describes the potential difference between the surface ($\Phi_{surf}$) and the bulk $\Phi_b$ (given by the doping of the semiconductor) and $\rho_0$ is the space charge density.
The space charge region leads on an electric field which counteracts further diffusion. Under the influence of this field, thermally generated minority charge carriers flow across the interface, which is the origin of the **generation current** $I_g$.
If no external voltage is applied, the recombination and generation current balance each other: $I_r(0) + I_g(0) = 0$.
Following the calculation of the space charge region at the semiconductor-vacuum interface, we can calculate the width w of the space charge region at the pn-junction based on the Poisson-equation under the assumption that the transition between p- and n-region is abrupt:

$$\omega = \sqrt{\frac{2\epsilon\epsilon_0}{e}\frac{N_A + N_D}{N_A \cdot N_D} \cdot U_D} \tag{2.34}$$

with $U_D$ the electrostatic potential at the interface (built-in potential).

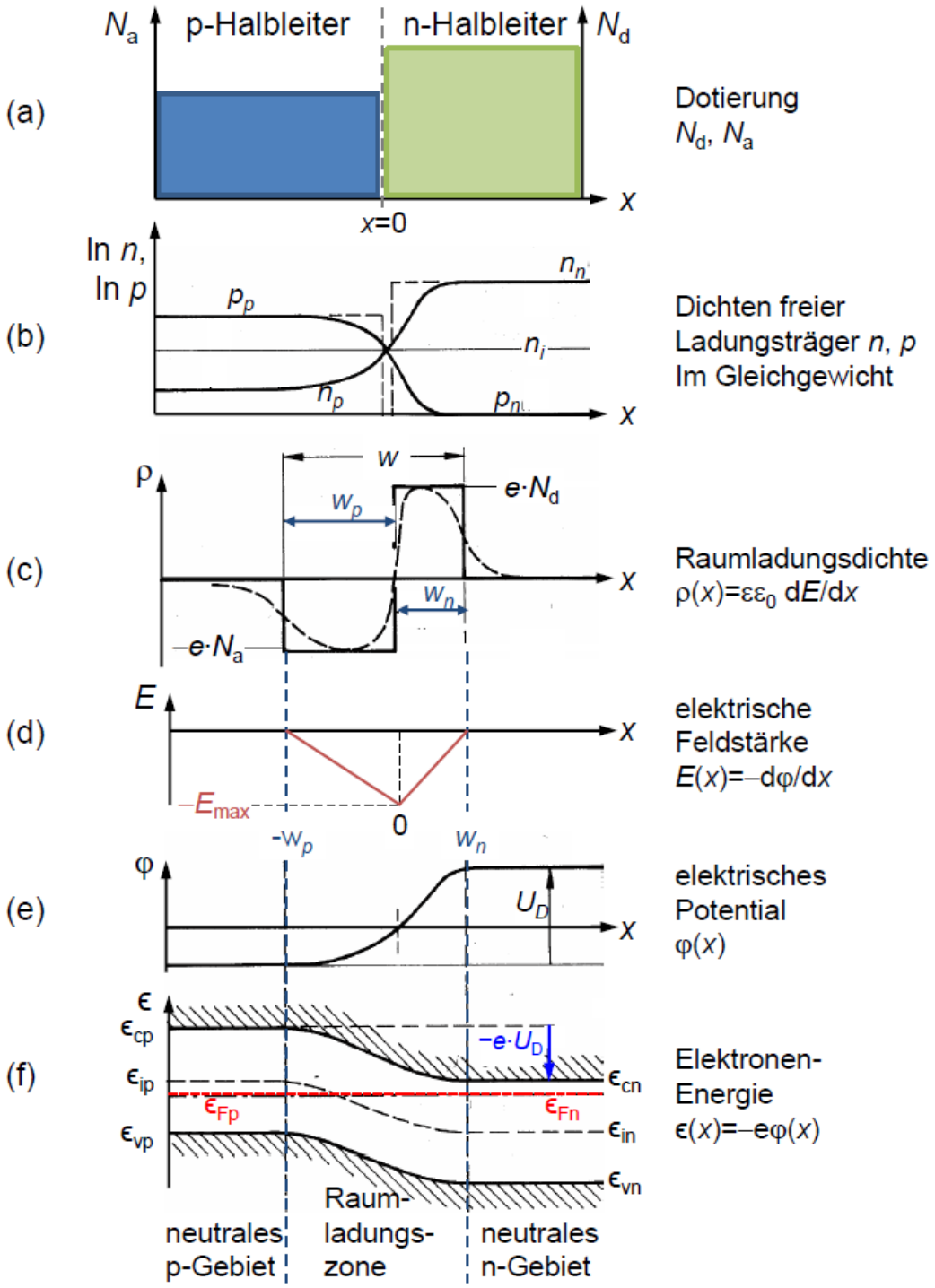


Fig. A.9: Abrupter *pn*-Übergang (schematisiert). Ortsverläufe verschiedener Größen für den Gleichgewichtsfall [nach Bergmann-Schaefer, Lehrbuch der Experimentalphysik, Bd. 6, Festkörper (1992); Abb.6.41].

**Strom-Spannungs-Kennlinie**

Bislang betrachteten wir den pn-Kontakt ohne äußere Spannung $U$.
In diesem Fall stehen Rekombinationsströme $I_r$ und Generationsströme $I_g$ im Gleichgewicht $\Rightarrow$ Nettostrom =0.

Im Fall eines endlichen Spannungsabfalls über den Kontakt:
$U > 0$ am $p$-Kontakt $\rightarrow$ erniedrigt Potentialbarriere $-e(U_D - |U|)$
$U < 0$ am $p$-Kontakt $\rightarrow$ erhöht Potentialbarriere $-e(U_D + |U|)$

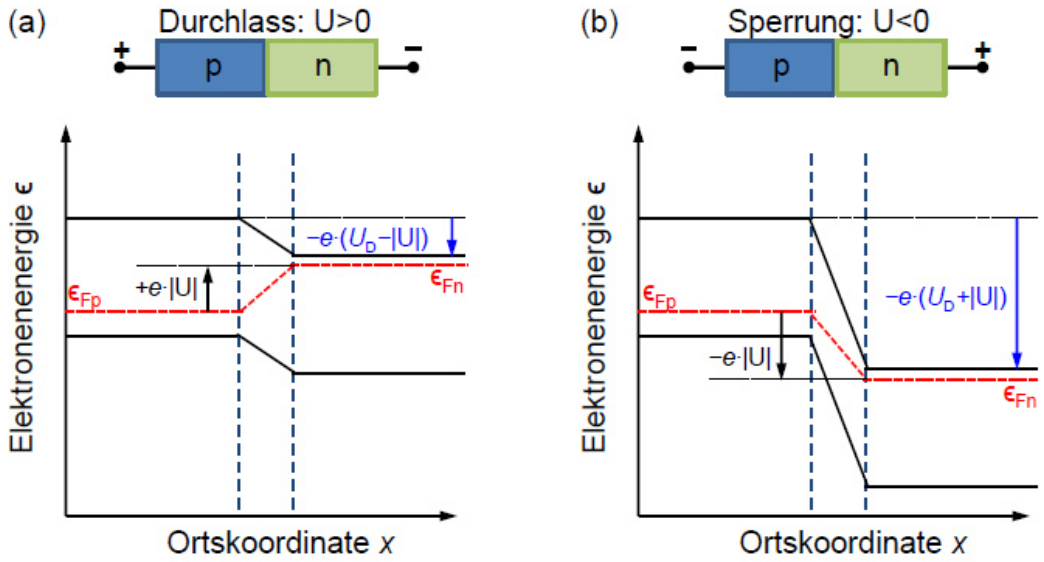


Fig. A.10: Energiebändermodell eines $pn$-Übergangs: (a) Durchlass; (b)Sperrung.

Auswirkung auf Rekombinations- und Generationsströme:

Rekombinationsströme: fließen gegen Barriere
skalieren exponentiell mit Barrierenhöhe (Boltzmann-Faktor !)

Elektronen: $n \rightarrow p$ $\quad I_{nr}(U) = I_{nr}(0)e^{eU/k_BT}$ mit $I_{nr}(0) > 0$
Löcher: $p \rightarrow n$ $\quad I_{pr}(U) = I_{pr}(0)e^{eU/k_BT}$ mit $I_{pr}(0) > 0$ (A.45)

Generationsströme: unabhängig von $U$ (erreichen immer andere Seite)

thermisch generierte Minoritätsladungsträger
$$I_{ng}(U) = I_{ng}(0) = -I_{nr}(0)$$
$$I_{pg}(U) = I_{pg}(0) = -I_{pr}(0) \qquad \text{(A.46)}$$

$\Rightarrow$ Gesamtstrom

$$\begin{aligned} I_{ges} &= I_{nr} + I_{ng} + I_{pr} + I_{pg} \\ &= I_{nr}(0)e^{eU/k_BT} - I_{nr}(0) + I_{pr}(0)e^{eU/k_BT} - I_{pr}(0) \\ &= I_{nr}(0)[e^{eU/k_BT} - 1] + I_{pr}(0)[e^{eU/k_BT} - 1] \\ &= \underbrace{\{I_{nr}(0) + I_{pr}(0)\}}_{\equiv I_0}[e^{eU/k_BT} - 1] \end{aligned} \qquad \text{(A.47)}$$

(wie beim Schottky-Kontakt)

**Sperrrichtung** ($U < 0$): Generationsstrom überwiegt,
geht für große Sperrspannung gegen $-I_0$ (Sättigungssperrstrom)

hier: Strom infolge Generation von Minoritätsladungsträgern
Schottky-Kontakt: thermische Emission der Elektronen von Metall zu Halbleiter über Barriere

Sättigungssperrstrom ist $T$-abhängig $\rightarrow$ $T$-Sensor (Si-Diode)

**Durchlassrichtung** ($U > 0$): Rekombinationsstrom überwiegt
skaliert exponentiell $\propto e^{eU/k_BT}$ für große Durchlassspannung

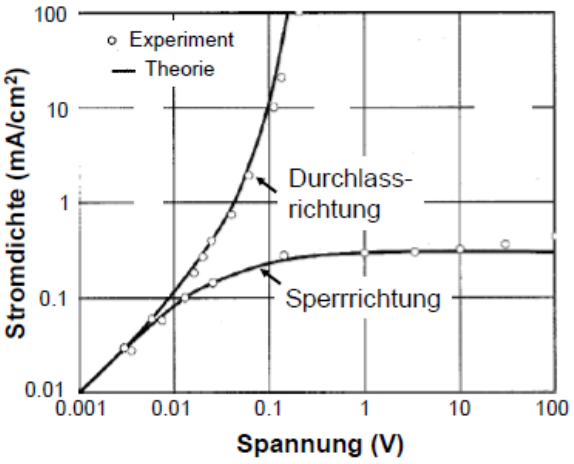


Fig. A.11: Gleichrichtungscharakteristik eines $p-n$-Überganges in Germanium, nach Shockley. [nach Ch. Kittel, Einführung in die Festkörperphysik (1999); Abb.19.14].

**Durchbruch:**

Elektrisches Feld in RLZ ist so groß, dass $E_{kin} > E_g \Rightarrow$ Erzeugung von $e^-$-Loch-Paaren;
$U > U_{Br}$: jeder eintretende Ladungsträger macht Stoßionisation $\Rightarrow$ Lawinendurchbruch

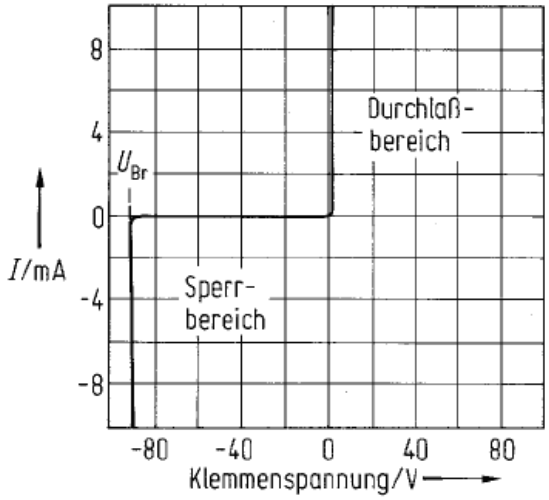


Fig. A.12: Strom-Spannungs-Kennlinie einer Siliziumdiode ($T = 300\,\mathrm{K}$) [aus Bergmann-Schaefer, Lehrbuch der Experimentalphysik, Bd. 6, Festkörper (1992); Abb.6.43].

#### 2.2.4.1 Current-voltage characteristics of a pn-junction

The current-voltage characteristics of the pn-junction can be understood following the discussion of the Schottky-barrier.

1. No external voltage ($U = 0$):

   Recombination and generation current cancel each other.

   $I = 0$

2. $U > 0$ on p-side:

   Potential barrier reduced to $-e(U_D - |U|)$

   The recombination current scales exponentially with the height of the barrier: $I_{nr}(U) = I_{nr}(0)e^{eU/kT}$ and $I_{pr}(U) = I_{pr}(0)e^{eU/kT}$

   The generation current is independent of the barrier.

   The total current is: $I_{tot}(U) = \{I_{nr}(0) + I_{pr}(0)\}\left[e^{eU/kT} - 1\right]$

   The behaviour is dominated by the recombination current, which scales exponentially with $eU$ for large $U$.

3. $U < 0$ on p-side:

   Potential barrier increased to $-e(U_D + |U|)$

   The behaviour is dominated by the generation current and approaches $-(I_{nr}(0) + I_{pr}(0))$ for large U (saturation current).

   This saturation current is due to the diffusion of minority charge carriers under the influence of the electric field at the interface. In case of the Schottky contact, the saturation current is caused by thermionic emission of electrons from the metal to the semiconductor.

   The saturation current is temperature-dependent.